1398–1404 *Nucleic Acids Research, 1999, Vol. 27, No. 5* *© 1999 Oxford University Press*

Unusual nucleotide conformations in GNRA and UNCG type tetraloop hairpins: evidence from Raman markers assignments

Nicolas Leulliot, Vladimir Baumruk[1], Mouhiba Abdelkafi, Pierre-Yves Turpin, Abdelkader Namane[2], Catherine Gouyette[2], Tam Huynh-Dinh[2] and Mahmoud Ghomi*

Laboratoire de Physicochimie Biomoléculaire et Cellulaire, UPRESA 7033, Université Pierre et Marie Curie, Case 138, 4 Place Jussieu, 75252 Paris Cedex 05, France, [1]Institute of Physics, Charles University, Ke Karlovu 5, 12116 Prague 2, Czech Republic and [2]Unité de Chimie Organique, URA CNRS 487, Institut Pasteur, 28 rue du Docteur Roux, 75724 Paris Cedex 15, France

Received September 9, 1998; Revised December 18, 1998; Accepted January 10, 1999

ABSTRACT

High resolution NMR data on UNCG and GNRA tetraloops (where N is any of the four nucleotides and R is a purine) have shown that they contain ribonucleosides with unusual 2′-*endo*/*anti* and 3′-*endo*/*syn* conformations, in addition to the 3′-*endo*/*anti* ones which are regularly encountered in RNA chains. In the current study, Raman spectroscopy has been used to probe these nucleoside conformations and follow the order (hairpin) to disorder (random chain) structural transitions in aqueous phase in the 5–80°C temperature range. Spectral evolution of GCAA and GAAA tetraloops, as formed in very short hairpins with only three G·C base pairs in their stems (T_m > 60°C), are reported and compared with those previously published on UUCG and UACG tetraloops, for which the *syn* orientation of the terminal guanine as well as the 2′-*endo*/*anti* conformation of the third rC residue have been confirmed by means of vibrational marker bands. Raman data obtained as a function of temperature show that the first uracil in the UUCG tetraloop is stacked and the two middle residues (rU and rC) are in the 2′-*endo*/*anti* conformation, in agreement with the previously published NMR results. As far as the new data concerning the GNRA type tetraloops are concerned, they lead us to conclude that: (i) in both cases (GCAA and GAAA tetraloops) the adenine bases are stacked; (ii) the second rC residue in the GCAA tetraloop has a 3′-*endo*/*anti* conformation; (iii) the sugar pucker associated with the third rA residue in both tetraloops possibly undergoes a 3′-*endo*/2′-*endo* interconversion as predicted by NMR results; (iv) the stem adopts a regular A-form structure; (v) all other nucleosides of these two GNRA tetraloops possess the usual 3′-*endo*/*anti* conformation.

INTRODUCTION

RNA hairpins represent structural fragments that allow RNA to fold back onto itself giving rise to its particular secondary and tertiary structures. Hairpins consist of an intramolecular double helix (stem) capped by a certain number of unpaired nucleotides (loop). In rRNAs, the majority of the loops include four ribonucleotides (tetraloops). It has been shown that >70% of these tetraloops belong to the GNRA and UNCG families (N = U, A, C or G, R = G or A) (1,2). Furthermore, one can recall some of the biological functions of GNRA and UNCG tetraloops: UUCG is the terminal site of reverse transcriptase action (3), whereas GAAA participates in long-range tertiary interactions in catalytic RNAs (4). In addition, it has been shown that UNCG and GNRA tetraloops, owing to their particular structural features, are unusually stable, provided that their stems include at least two G·C base pairs, preferentially with a C·G one closing the tetraloop (5–11). Thus, short hairpins with a comparable number of ribonucleotides in the loop and in the stem can easily be formed in aqueous phase. This is extremely important for spectroscopic techniques (NMR and vibrational spectroscopies) used to probe the structural features of these systems, because the signals arising from the loop ribonucleotides are not completely hidden by those arising from the stem.

High resolution NMR data were recently published on UUCG (11–16), UACG (10,17), GAAA and GCAA (18–20) tetraloop hairpins formed in aqueous solutions of oligoribonucleotides. These data explain the unusual stability of these tetraloops by the following structural peculiarities: (i) U·G and G·A mismatch pairs formed between the first and the last bases of UNCG and GNRA tetraloops, respectively (Fig. 1); (ii) stacking of the third unpaired loop base with another base of the loop; (iii) stabilising intramolecular H-bonds within the tetraloop. In both families of tetraloops, the second base is looped-out (stacked or unstacked with other bases). As far as the fine structure of the ribonucleotides in the loops and stems is concerned, NMR data have proved that the stem forms an ordered A-form intramolecular double helix

*To whom correspondence should be addressed. Tel: +33 1 4427 7555; Fax: +33 1 4427 7560; Email: ghomi@lpbc.jussieu.fr

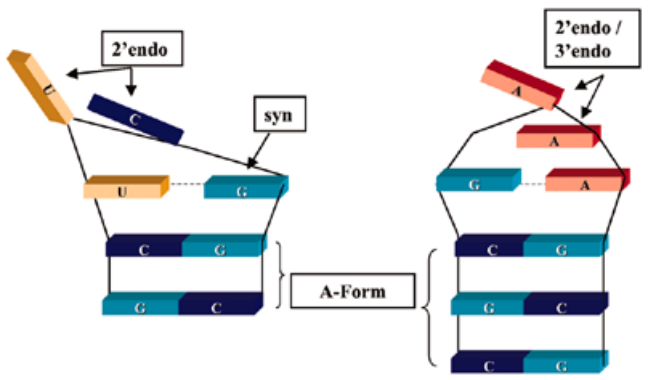

Figure 1. Schematic relative positions of the base residues in UUCG and GAAA tetraloop hairpins as predicted from restrained molecular modelling based on NMR data, taken from Cheong *et al.* (12) and Nowakowski and Tinoco (17), respectively. Stems form intramolecular A-form double helices. All the nucleosides are in the 3′-*endo*/*anti* conformation unless indicated otherwise.

whatever its base composition is. In both the UUCG (11–16) and UACG (10,17) tetraloops, the middle ribonucleosides adopt a 2′-*endo*/*anti* conformation, while the last rG has a 3′-*endo*/*syn* conformation. In aqueous phase, all the bases in the GAAA and GCAA tetraloops adopt an *anti* orientation versus the sugar, while the sugar puckers involved in the two middle ribonucleotides undergo possible 3′-*endo*/2′-*endo* interconversion (18–20).

Vibrational spectroscopy has also proven its efficiency to probe nucleotide structural features in nucleic acids (21–31). It should be reminded that Raman marker bands have indeed been documented for a great variety of RNA and DNA structures (for reviews see refs 30,31 and our recent papers on UNCG tetraloops, 9–11). In addition, many of the previous experiments on ribonucleosides, ribonucleotides and polyribonucleotides (not shown here) have also been repeated to ensure consistency with the present experiments. Beyond the pioneering investigations on synthetic polyribonucleotides establishing the most prominent spectral characteristics arising from ordered single or double helical A-form RNA chains (21–25), which generally constitute the most favourable conformations of these systems in aqueous solutions, the success in obtaining the Z-form Raman spectra under special physicochemical conditions (presence of counter-ions, temperature) should be emphasised. A-form to Z-form double helical transitions have been monitored in poly r(G-C) (26) and $r(C\text{-}G)_3$ (27) by non-resonance Raman spectroscopy and in poly r(A-U) (28) by UV resonance Raman spectroscopy and then confirmed by the observation of substantial changes in UV circular dichroism spectra (26,28). The most interesting results are basically related to the fact that in Z-RNA chains, as formed by alternating purine–pyrimidine sequences, unusual 2′-*endo*/*anti* pyrimidine and 3′-*endo*/*syn* purine ribonucleosides can be found, instead of the usual 3′-*endo*/*anti* conformation characteristic of A-form helices. In parallel, the presence of a Z-form RNA double helix in aqueous solutions has also been evidenced by ^{1}H and ^{31}P NMR spectroscopy (26).

The aim of this work is to demonstrate to what extent vibrational spectroscopy can be applied to probe unusual nucleoside conformations in GNRA and UNCG tetraloop hairpins. Raman spectra obtained at various temperatures, revealing the evolution of the nucleotide vibrational markers in going from an ordered (hairpin) to a disordered (random chain) structure, are reported.

MATERIALS AND METHODS

Chemical synthesis

All the oligomers used for recording UV absorption and Raman spectra were able to form UNCG and GNRA tetraloop hairpins. Approximately 3–4 mg of 5′-r[GC-UUCG-GC]-3′, 5′-r[GC-UACG-GC]-3′ octamers and 5′-r[CGC-GAAA-GCG]-3′, 5′-r[CGC-GCAA-GCG]-3′ decamers were synthesised following the chemical procedure described previously (10). Hereafter, for the sake of brevity, these oligomer sequences are referred to as UUCG, UACG, GAAA and GCAA tetraloop hairpins, respectively.

Sample preparation and experimental conditions

Lyophilised oligomer samples containing one Na^{+} ion per phosphate group were dissolved in 10 mM phosphate buffer, pH 7, with 0.1 mM EDTA. Final oligomer concentration in aqueous solution was 40 µM and 1 mM for UV absorption and 10 mM for Raman spectroscopy.

Experimental set-up and details concerning UV absorption and Raman scattering measurements are identical to those previously used for UUCG and UACG hairpins (9,10). Raman spectra were obtained with the excitation at 514.5 nm emitted from an argon laser (with ~150 mW of radiant power at the sample). The temperature gradient across the sample cell was <0.5°C. It should be noted that although Raman spectra were recorded for higher concentrations than those used in UV absorption measurements, we have encountered no evidence for intermolecular association. Reversibility of structural transitions (hairpin to disordered and/or disordered to hairpin) has been verified by gradually heating the samples from 5°C to the highest temperature limit (~80°C) and cooling down to 20°C. Raman spectra taken at 20°C before and after the thermal annealing were particularly superimposable. On the other hand, by following the evolution of Raman spectra as a function of temperature, we could conclude that they cannot be interpreted as a superposition of those arising from different molecular species. The changes observed in Raman spectra as a function of temperature follow the behaviour predicted by UV absorption melting profiles confirming a hairpin to random chain transition. To compare the relative intensities of the various Raman spectra, the band at ~1095 cm^{-1}, corresponding to the PO_2^{-} symmetric stretching mode, has been used as an internal intensity standard. For each oligomer, Raman spectra were obtained at each 5°C temperature step. So we have controlled the validity of taking the 1095 cm^{-1} Raman band as an internal reference by following its slight wavenumber shift and profile as a function of temperature. This careful procedure could lead us to a very precise overall normalisation of the spectra and made possible a comparison between Raman spectra obtained at the two ultimate temperatures. Raman spectra obtained from the four different oligomers were first normalised in order to get the same height for the internal reference. Then, as these oligomers do not possess the same number of phosphate groups (seven in octamers

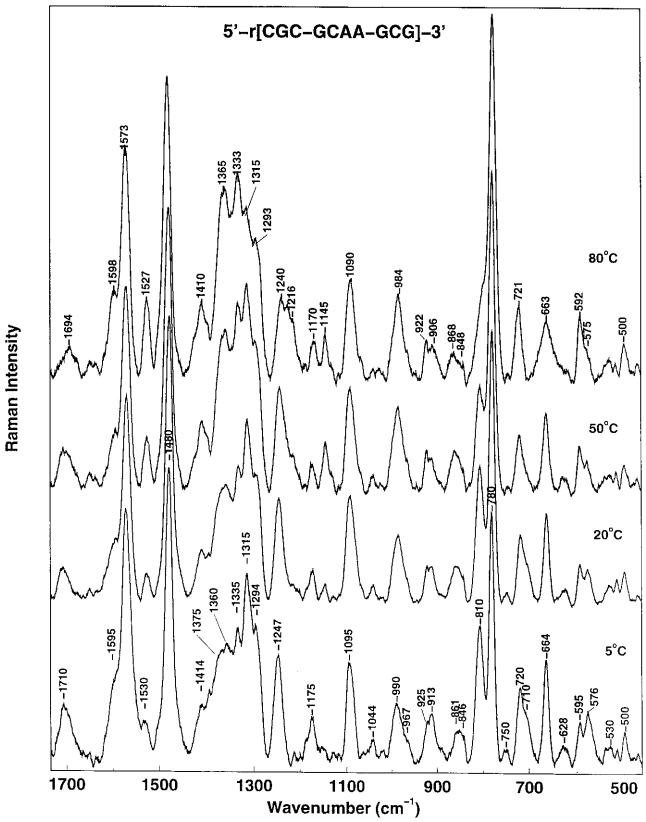

Figure 2. Evolution of the Raman spectra (λ_{exc} = 514.5 nm) of the 5′-r[CGC-GCAA-GCG]-3′ decamer in H_2O buffer as a function of the temperature (5–80°C) in the 1725–450 cm^{-1} spectral range. Spectra were normalised to the $\nu_s(PO_2^-)$ band at ~1095 cm^{-1} as an internal standard.

versus nine in decamers), the octamer Raman spectra have been multiplied by a correction factor equal to 0.78 (= 7/9).

RESULTS AND DISCUSSION

Thermodynamic stability of the hairpins

In all cases, melting profiles obtained at 40 µM and 1 mM concentrations can be perfectly superimposed and show a unimolar, progressive and reversible hairpin to random chain transition. The melting profiles of the UNCG hairpins have been published previously (10,11). Those of GAAA and GCAA (results not shown) show the same behaviour. The T_m values of the studied hairpins were found in the following decreasing order: 64 (GAAA), 62 (GCAA), 54 (UUCG) and 51°C (UACG), confirming their unusually high thermal stability.

Raman spectra

In order to show the progressive evolution of the vibrational spectral bands with temperature, when going from ordered to disordered conformers, the GCAA decamer Raman spectra, recorded at four different temperatures located respectively well below (5 and 20°C), close to (50°C) and well above (80°C) the T_m value of this hairpin, are displayed in Figure 2.

Comparison between the Raman spectra obtained at the two ultimate temperatures (i.e. 5 and 80°C) for the four hairpins has been carried out in two different spectral regions, i.e. 1735–1150 and 1125–600 cm^{-1}, as displayed in Figures 3 and 4, respectively. Detailed spectral evolution of UUCG and UACG hairpins with temperature have been reported recently (9,10). Positions of Raman bands, corresponding to hairpin tetraloops observed at low temperature, as well as their assignments based on previous studies, are summarised in Table 1.

1735–1150 cm^{-1} spectral region. In this spectral region, vibrational modes arising mainly from nucleic acid bases occur. Below 1400 cm^{-1}, a number of vibrational modes also carry valuable information on the sugar pucker conformation through coupling between the base and sugar vibrational motions. Observed changes in some of these vibrational modes with increasing temperature allowed us to make the following assumptions.

(i) The interbase hydrogen bonds are disrupted in all cases with increasing temperature. This process can be monitored by gradual disappearance of the band at 1710 cm^{-1} arising from carbonyl stretching motion, that is downshifted to 1686 cm^{-1} at high temperature. Other minor changes in the 1675–1640 cm^{-1} spectral region also reinforce this assignment (Fig. 3).

(ii) The rG residue at the last position of UUCG and UACG tetraloops adopts a 3′-*endo*/*syn* conformation, as shown by appearance of a sharp band at 1320 cm^{-1}, whose intensity decreases considerably with increasing temperature (Fig. 3a and b). A weaker shoulder observed at 1315 cm^{-1} corresponds to the 3′-*endo*/*anti* conformation of the rG residues of the stem (as observed in the Raman spectra of single and double A-form strands). Only a single band at 1315 cm^{-1}, corresponding to the 3′-*endo*/*anti* rG residues involved in both loop and stem, is observed in Raman spectra of both GAAA and GCAA hairpins (Fig. 3c and d).

(iii) The rA residues involved in GCAA and GAAA tetraloops are stacked at low temperature: this is reflected in hypochromism of Raman bands at 1335 and 1375 cm^{-1} (Fig. 3c and d). On the other hand, since the UACG tetraloop contains only one adenine in the tetraloop, it is rather difficult to detect intensity changes of the rA modes, because they are mostly superimposed with the more pronounced rG modes (Fig. 3b).

(iv) All rC residues involved in both GAAA and GCAA hairpins are found in 3′-*endo*/*anti* conformations: this is confirmed by the presence of the conformation marker band at ~1250 cm^{-1} (Fig. 3c and d). This band has been reported in the spectra of A-form double-stranded helices (23,24), containing only 3′-*endo*/*anti* nucleosides. No extra shoulder at ~1265 cm^{-1} revealing the existence of a 2′-*endo*/*anti* rC residue in the GCAA tetraloop loop has been observed (Fig. 3d; see also below for more details in the case of the UUCG and UACG tetraloops).

Table 1. Wavenumbers (cm^{-1}) and assignment of the most prominent Raman bands observed in Raman spectra of various hairpins at 5°C

UUCG hairpin[a]	UACG hairpin[b]	GAAA hairpin[c]	GCAA hairpin[d]	Assignment
1710 (sh)	1710 (w)	1710 (w, br)	1710 (w, br)	base C=O; stem
1686 (m, br)	1686 (w, br)			base C=O; stem and loop
1670 (sh)	1670 (sh)			base double-bond; stem and loop
1595 (m)	1595 (sh)	1595 (sh)	1595 (sh)	r(C); 3′-*endo*/*anti*; stem
1574 (vs)	1573 (s)	1573 (vs)	1573 (vs)	r(G); stem and loop
1530 (w)	1530 (w, br)	1530 (vw, br)	1530 (w, br)	r(C); 3′-*endo*/*anti*; stem
		1503 (sh)	1503 (sh)	r(A); loop
1481 (vs)	1481 (vs)	1480 (vs)	1480 (vs)	r(G); stem and r(A); loop
1417 (m)	1417 (w)	1414 (m)	1414 (sh)	r(G); stem and loop
1381 (m, br)	1381 (m)	1375 (m)	1375 (sh)	r(A); 3′-*endo*/*anti*; stem and loop,
				r(G); 3′-*endo*/*anti*; stem and loop
1359 (m, br)	1359 (m)	1360 (sh)	1360 (s)	r(G); 3′-*endo*/*anti*; loop and stem
	1335 (sh)	1335 (s)	1335 (s)	r(A); loop
1321 (vs)	1321 (vs)			r(G); 3′-*endo*/*syn*; loop
		1315 (vs)	1315 (vs)	r(G); 3′-*endo*/*anti*; stem and loop
1294 (m)	1300 (m)	1294 (sh)	1294 (s)	r(C); 3′-*endo*/*anti*; stem and loop
				r(A) loop
1263 (sh)	1263 (sh)			r(C); 2′-*endo*/*anti*; loop
1250 (sh)	1250 (sh)	1250 (s)	1247 (s)	r(C); 3′-*endo*/*anti*; loop and stem
1235 (vs)	1237 (s)			r(U); loop
1185 (w)	1185 (w)	1176 (w)	1175 (w)	r(G); stem and loop
1095 (m)	1095 (m)	1095 (m)	1095 (m)	PO_2^- symmetric stretch
1044 (w, br)	1044 (w, br)	1043 (w, br)	1044 (vw, br)	backbone, ribose
997 (vw, br)	999 (w)	990 (w, br)	990 (w, br)	backbone
973 (vw, br)	973 (vw, br)			backbone
925 (w)		925 (m)	925 (sh)	backbone
916 (sh)	916 (vw, br)	912 (sh)	913 (w)	backbone
880 (vw, br)	880 (vw, br)			backbone
868 (vw, br)	868 (vw, br)	862 (vw, br)	861 (vw, br)	phosphate–backbone
848 (vw, br)	850 (vw, br)	846 (vw, br)	846 (vw, br)	phosphate–backbone
810 (s)	810 (s)	810 (s)	810 (s)	O-P-O symmetric stretch (A marker)
783 (vs)	785 (vs)	782 (vs)	780 (vs)	r(C) breathing mode; stem and loop;
				r(U) breathing mode; loop
	725 (w)	724 (m)	720 (m)	r(A) breathing mode; loop
710 (w)	715 (w)	710 (sh)	710 (sh)	backbone; stem (A marker)
671 (w)	671 (w)	665 (s)	664 (s)	r(G); 3′-*endo*/*anti*; loop and stem
636 (w)	636 (w)			r(G); 3′-*endo*/*syn*; loop

vs, very strong; s, strong; m, medium; w, weak; vw, very weak; br, broad; sh, shoulder.
[a]As formed in aqueous solutions of 5′-r[GC-UUCG-GC]-3′ octamer (Figs 3a and 4a).
[b]As formed in aqueous solutions of 5′-r[GC-UACG-GC]-3′ octamer (Figs 3b and 4b).
[c]As formed in aqueous solutions of 5′-r[CGC-GAAA-GCG]-3′ decamer (Figs 3c and 4c).
[d]As formed in aqueous solutions of 5′-r[CGC-GCAA-GCG]-3′ decamer (Figs 3d and 4d).

(v) The first rU residue in both UUCG and UACG tetraloops is stacked in agreement with the NMR results in these cases (10–17). This can be observed by a rapid review of the intensity of the Raman band at ~1235 cm^{-1} which presents a remarkable hypochromism in both UUCG and UACG tetraloops (Fig. 3a and b). This effect has also been observed in Raman spectra of poly rU

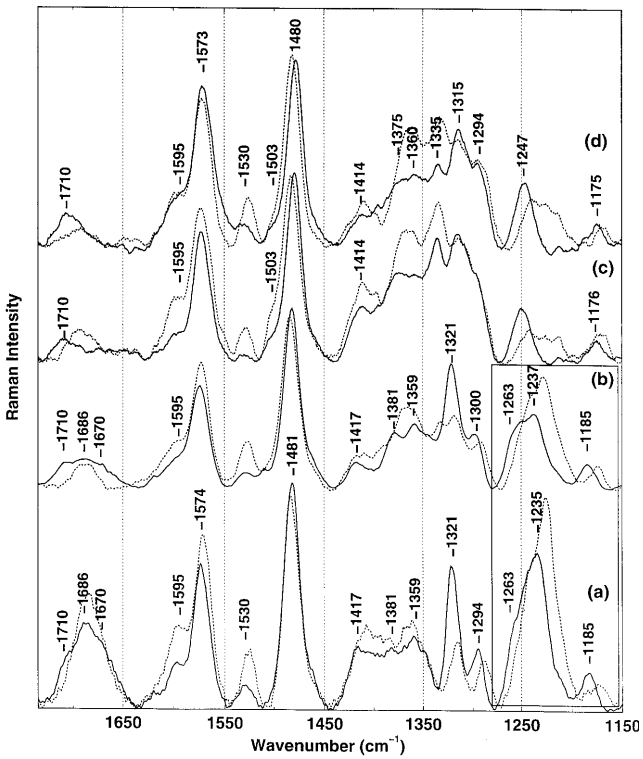

Figure 3. Comparison of Raman spectra (λ_{exc} = 514.5 nm) of (**a**) 5′-r[GC-UUCG-GC]-3′, (**b**) 5′-r[GC-UACG-GC]-3′, (**c**) 5′-r[CGC-GAAA-GCG]-3′ and (**d**) 5′-r[CGC-GCAA-GCG]-3′ oligomers in the 1735–1150 cm^{-1} spectral range recorded at 5 (solid line) and 80°C (dotted line). See Materials and Methods for description of the normalisation procedure. Wavenumber labels correspond to peak intensities observed in low temperature (solid line) spectra. The framed overlapped bands in the 1275–1150 cm^{-1} region in spectra (c) and (d) have been subjected to a band decomposition with Lorentzian components as displayed in Figure 5.

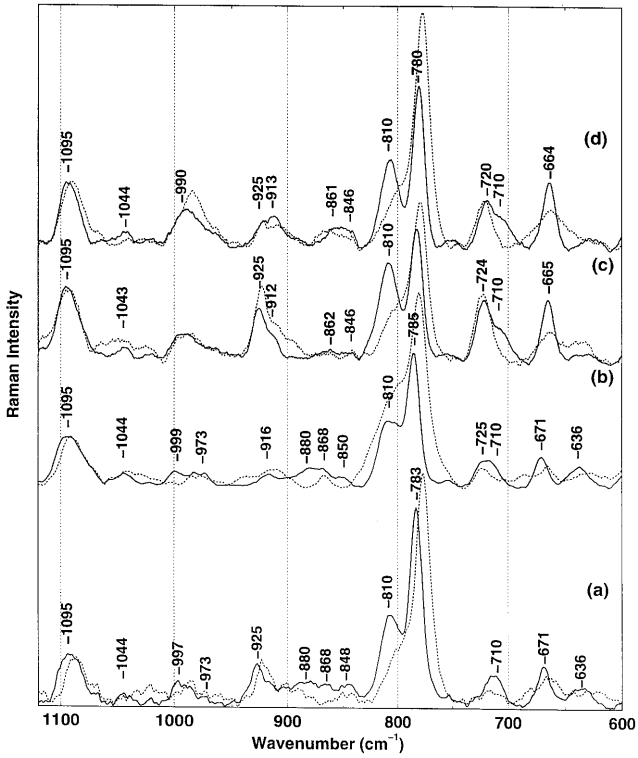

Figure 4. Comparison of Raman spectra (λ_{exc} = 514.5 nm) of (**a**) 5′-r[GC-UUCG-GC]-3′, (**b**) 5′-r[GC-UACG-GC]-3′, (**c**) 5′-r[CGC-GAAA-GCG]-3′ and (**d**) 5′-r[CGC-GCAA-GCG]-3′ oligomers in the 1120–600 cm^{-1} spectral range recorded at 5 (solid line) and 80°C (dotted line). See Materials and Methods for description of the normalisation procedure. Wavenumber labels correspond to peak intensities observed in low temperature (solid line) spectra.

(21). However, it should be noted that this band is located in a spectral region (1275–1200 cm^{-1}) where a set of overlapped bands exists which arises from rC and rU residues included in the UNCG hairpins (framed in Fig. 3). To overcome this difficulty and in order to give a more reliable assignment to the observed bands in this region, we have undertaken a band decomposition as shown in Figure 5 with a reasonable number of bands (as well as their half-widths) at low and high temperatures. As shown in Figure 5, three components have been proposed at low temperature while only two components exist at high temperature, because the component at 1263 cm^{-1} disappears with increasing temperature in agreement with a hairpin to random chain conformational transition. This band is assigned to the rC residue located at the third position of the UUCG and UACG tetraloops that adopts the 2′-*endo*/*anti* conformation, as supported by Raman spectra of poly r(G-C) and r(G-C)$_3$ in the Z-form that contains 2′-*endo*/*anti* pyrimidine residues (26,27). The intensity of the other two components (at 1250 and 1235 cm^{-1}) found in this decomposition increase in going to high temperature. As mentioned above, the 1250 cm^{-1} component arises mainly from the stem 3′-*endo*/*anti* rC. Another effect emerging from this band decomposition is that at low temperature the intensity of the component at 1250 cm^{-1} is more important in the UUCG hairpin (Fig. 5b) than in the UACG (Fig. 5a) hairpin. Thus in the case of the UUCG tetraloop the assignment of this band solely to the 3′-*endo*/*anti* rC nucleosides becomes rather difficult, because both the UUCG and UACG hairpins have the same number of rC residues. Thus, we conclude that the component at 1250 cm^{-1} might include a contribution arising from the rU residue in the second position of the tetraloop. To be sure of this assignment, we have used our recent *ab initio* calculations on the rU residues in both the 2′-*endo*/*anti* and 3′-*endo*/*anti* conformations (results to be published). Harmonic vibrational calculations at the DFT/B3LYP/6-31G* level of theory show that this characteristic mode of the rU residue undergoes a +10 cm^{-1} shift on 3′-*endo*/*anti*→2′-*endo*/*anti* conformational transition. Thus, the intense rU Raman band at 1235 cm^{-1} assigned to the 3′-*endo*/*anti* conformation should shift up to ~1250 cm^{-1} when this residue adopts a 2′-*endo*/*anti* conformation and becomes superimposed with the characteristic Raman band of the rC residue in the 3′-*endo*/*anti* conformation appearing around the same wavenumber. This fact allows us to interpret unambiguously the change in the intensity of the 1250 cm^{-1} Raman band from the UACG to UUCG hairpins (Fig. 5). It is worth noting that this band decomposition associated with quantum mechanical calculations confirms the NMR data (12), which assumed that the rU residue at the second position of the loop is in the 2′-*endo*/*anti* conformation (Fig. 1).

1120–600 cm^{-1} spectral region. The ordered structure in RNAs and especially the formation of an A-form helix is generally

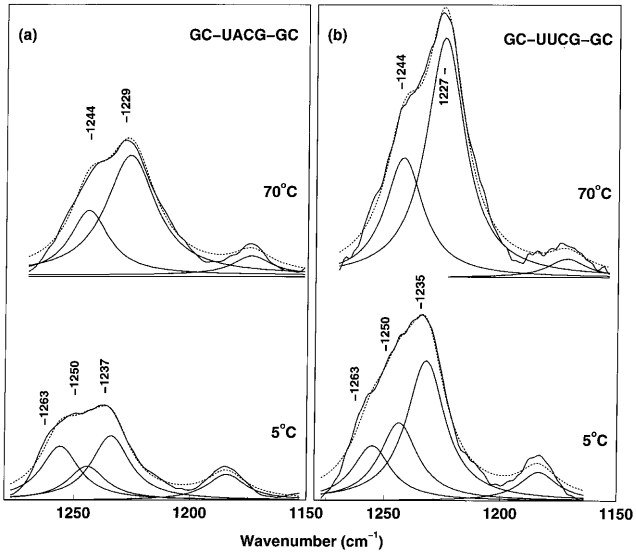

Figure 5. Band decomposition of Raman spectra (λ_{exc} = 514.5 nm) of (**a**) 5′-r[GC-UACG-GC]-3′ and (**b**) 5′-r[GC-UUCG-GC]-3′ in the 1275–1150 cm^{-1} spectral region at 5 (bottom) and 70°C (top). recorded at 5 (solid line) and 80°C (dotted line). All of these spectra were normalised to the $\nu_s(PO_2^-)$ band at ~1095 cm^{-1} as an internal standard, leading to a comparable intensity scale. Spectra drawn with dotted lines represent the sum of the Lorentzian component bands introduced in the decomposition procedure. General half-width for all these bands was ~20 cm^{-1}.

confirmed by the presence of a Raman marker band at ~810 cm^{-1} (21–27). In low temperature Raman spectra of all studied hairpins the band at 810 cm^{-1} is observed (Fig. 4), that vanishes progressively with increasing temperature, confirming melting of the short A-form helical stem of each hairpin (Fig. 4). The disappearance of a weak 710 cm^{-1} line also indicates the transition of the hairpins towards random chains (21–25). A band at 665 cm^{-1} (Fig. 4c and d), the marker band for the 3′-*endo*/*anti* rG residues (26–27), as well as that found at 636 cm^{-1} (only observed in UUCG and UACG hairpins; Fig. 4a and b), the marker band for the 3′-*endo*/*syn* rG residue of the loop (26–27), become weaker and give rise to a broad and diffuse band in high temperature spectra: this also proves the loss of ordered structure of the rG residues (29).

CONCLUDING REMARKS

Many attempts in classical molecular modelling, including molecular mechanics (12,14,18,19), molecular dynamics (32) and Monte Carlo–Metropolis (10), have revealed the difficulties related to the exploration of acceptable structures on the basis of NMR constraints for these highly stable RNA tetraloops (UNCG and GNRA). We have shown that Raman and infrared spectroscopy jointly used with quantum mechanical calculations can be employed as complementary techniques to NMR and classical molecular modelling in order to probe conformation of individual ribonucleotides in short RNA hairpins having rather complex structures.

Raman marker bands arising from the rC residues in the 3′-*endo*/*anti* (1250 cm^{-1}) and 2′-*endo*/*anti* (1265 cm^{-1}) as well as those assigned to the rG residues in the 3′-*endo*/*anti* (1360, 1315 and ~665 cm^{-1}) and 3′-*endo*/*syn* (1320 with high intensity and 636 cm^{-1}) conformations have proved their efficiency for the purpose.

On the basis of careful analysis, we can now propose a 3′-*endo*/*anti* conformation for the rC residue at the second position of the GCAA tetraloop. However, an 830 cm^{-1} marker band observed in FTIR spectrum of GCAA (not shown) confirms the presence of a 2′-*endo* ribose in this tetraloop. This leads us to conclude that the sugar pucker associated with the rA residue at the third position of the GCAA tetraloop may undergo a 3′-*endo*/2′-*endo* interconversion as suggested from NMR results. The same FTIR marker band indicates the existence of 2′-*endo* sugar puckering in the GAAA tetraloop (spectrum not shown). This ribose conformation should correspond to one of the rA residues in the second or third position of the loop. Taking into account the similarity between the vibrational markers arising from the sugar–phosphate and nucleosides as well as the melting profiles, we can assume that the GAAA and GCAA tetraloops have common structural features. Consequently, this 2′-*endo*/*anti* conformational marker should also be assigned to the third rA residue of the GAAA tetraloop. However, a possible 3′-*endo*/2′-*endo* interconversion for the sugar puckers involved in the middle rA residues of this tetraloop (NMR data) cannot be completely ruled out.

On the other hand, the stacking of the first uracil residue in the UNCG tetraloops is confirmed by the Raman spectra. Moreover, on the basis of the Raman band decomposition associated with quantum mechanical calculations, a 2′-*endo*/*anti* conformation for the second rU residue in the UUCG tetraloop is found, in agreement with NMR data.

ACKNOWLEDGEMENTS

Professor Jian-Sheng Sun from the Biophysics Laboratory of the Museum d'Histoire Naturelle (Paris) is gratefully acknowledged for recording the UV absorption spectra of GNRA hairpins. N.L. was supported by a PhD study grant from the MENESR. V.B. stayed in Paris during 1997 and 1998, thanks to fellowships from the French Ministry of Education, Ministry of Foreign Affairs and the UPMC. This work was supported by Project No. VS-97113 from the Czech Ministry of Education, Youth and Sports and by Barrande Project No. 98065.

REFERENCES

1 Woese,C.R., Winker,S. and Gutell,R.R. (1990) *Proc. Natl Acad. Sci. USA*, **87**, 8467–8471.
2 Uhlenbeck,O.C. (1990) *Nature*, **346**, 613–614.
3 Tuerk,C., Gauss,P., Thermes,C., Groebe,D.R., Gayle,M., Guild,N., Stromo,G., d'Aubenton-Carafa,Y., Uhlenbeck,O.C., Tinoco,I.,Jr, Brody,E.N. and Gold,L. (1988) *Proc. Natl Acad. Sci. USA*, **85**, 1364–1368.
4 Pley,H.W., Flaherty,K.M. and McKay,D.B. (1994) *Nature*, **372** 111–113.
5 Antao,V.P., Lai,S.Y. and Tinoco,I.,Jr (1991) *Nucleic Acids Res*., **19**, 5901–5905.
6 Antao,V.P. and Tinoco,I.,Jr (1992) *Nucleic Acids Res*., **20**, 819–824.
7 SantaLucia,J.,Jr, Kierzek,R. and Turner,D.H. (1992) *Science*, **256**, 217–219.
8 Molinaro,M. and Tinoco,I.,Jr (1995) *Nucleic Acids Res*., **23**, 3056–3063.
9 Abdelkafi,M., Leulliot,N., Ghomi,M. Hervé du Penhoat,C., Namane,A., Gouyette,C. Huynh-Dinh,T., Baumruk,V. and Turpin,P.-Y. (1997) *J. Mol. Struct*., **409**, 241–245.
10 Abdelkafi,M., Ghomi,M., Turpin,P.-Y., Baumruk,V., Hervé du Penhoat,C., Lampire,O., Bouchemal-Chibani,N., Goyer,P., Namane,A., Gouyette,C., Huynh-Dinh,T. and Bednárová,L. (1997) *J. Biomol. Struct. Dyn*., **14**, 579–593.

11 Abdelkafi,M., Leulliot,N., Baumruk,V., Bednárová,L., Turpin,P.-Y. Namane,A., Gouyette,C., Huynh-Dinh,T. and Ghomi,M. (1998) *Biochemistry*, **37**, 7878–7884.
12 Cheong,C., Varani,G. and Tinoco,I.,Jr (1990) *Nature*, **346**, 680–68.
13 Sakata,T., Hiroaki,H., Oda,Y., Tanaka,T., Ikehara,M. and Uesugi,S. (1990) *Nucleic Acids Res*., **18**, 3881–3839.
14 Varani,G., Cheong,C. and Tinoco,I.,Jr (1991) *Biochemistry*, **30**, 3280–3289.
15 Varani,G. (1995) *Annu. Rev. Biophys. Biomol. Struct*., **24**, 379–404.
16 Allain,F.H.T. and Varani,G. (1995) *J. Mol. Biol*., **250**, 333–353.
17 Nowakowski,J. and Tinoco,I.,Jr (1996) *Biochemistry*, **35**, 2577–2585.
18 Heus,H.A. and Pardi,A. (1991) *Science*, **253**, 191–194.
19 Jucker,F.M., Heus,H.A., Yip,P.F., Moors,E.H.M. and Pardi,A. (1996) *J. Mol. Biol*., **264**, 968–980.
20 Orita,M., Nishikawa,F., Shiamayama,T. Taira,K., Endo,Y. and Nishikawa,S. (1993) *Nucleic Acids Res*., **21**, 5670–5678.
21 Small,E.W. and Peticolas,W.L. (1971) *Biopolymers*, **10**, 1377–1416.
22 Lafleur,L., Rice,J. and Thomas,G.J.,Jr (1972) *Biopolymers*, **11**, 2423–2437.
23 Brown,K.G., Kiser,E.J. and Peticolas,W.L. (1972) *Biopolymers*, **11**, 1855–1869.
24 Morikawa,K., Tsuboi,M., Takahashi,S., Kyogoku,Y., Mitsui,Y., Iitaka,Y. and Thomas,G.J.,Jr (1973) *Biopolymers*, **12**, 799–816.
25 Chou,C.H. and Thomas,G.J.,Jr (1977) *Biopolymers*, **16**, 765–789.
26 Trulson,M.O., Cruz,P., Puglisi,J.D., Tinoco,I.,Jr and Maties,R.A. (1987) *Biochemistry*, **26**, 8624–8630.
27 Nishimura,Y., Tsuboi,M., Uesugi,S., Ohkubo,M. and Ikehara,M. (1985) *Nucleic Acids Symp. Ser*., **16**, 25–28.
28 Tomkova,A., Chinsky,L., Miskovsky,P. and Turpin,P.-Y. (1994) *J. Mol. Struct*., **318**, 65–77.
29 Small,E.W., Brown,K.G. and Peticolas,W.L. (1972) *Biopolymers*, **11**, 1209–1215.
30 Thomas,G.J.,Jr and Wang,A.H.J. (1988) In Eckstein,F. and Lilley,D.M.J. (eds), *Nucleic Acids and Molecular Biology*, Vol. 12, *Laser Raman Spectroscopy of Nucleic Acids*. Springer Verlag, Berlin, Germany, pp. 1–29.
31 Peticolas,W.L. and Evertsz,E. (1992) *Methods Enzymol*., **211**, 334–352.
32 Miller,J.L. and Kollman,P.A. (1997) *J. Mol. Biol*., **270**, 436–450.